

Absorption Spectrum of Optically Pumped  $\text{Al}_2\text{O}_3:\text{Cr}^{3+}$ †

J. W. HUANG\* AND H. W. MOOS‡

*Department of Physics, The Johns Hopkins University, Baltimore, Maryland 21218*

(Received 7 August 1967; revised manuscript received 15 April 1968)

The absorption cross sections of the  $\text{Cr}^{3+}$  ion in the metastable states  ${}^2E$  ( $\bar{E}$  and  $2\bar{A}$ ) of lightly doped ruby ( $\sim 0.01\%$ ) have been measured as a function of polarization at temperatures of 30, 105, and 296°K in the region from 2300 to 7000 Å. The lifetime of these states was measured by observing the decay rate of the excited-state absorption, and agreed with the value of the measured fluorescence decay rate at various temperatures. The population of the excited states was measured by the change of the area under the first two vibronic sidebands at low temperatures. At room temperature the population was measured by the change of transmitted intensity of a ruby laser.

## I. INTRODUCTION

BECAUSE of the long lifetime of the lowest excited states of the  $\text{Cr}^{3+}$  in  $\text{Al}_2\text{O}_3$ , these states are highly populated under irradiation by intense light, and absorption spectra from these doublet states to higher doublet states are observable as strong lines.<sup>1-4</sup> Owing to the difference in the spin quantum number, these states would not normally be observable from the  ${}^4A_2$  ground state. The expected spectra have been discussed by Shinada *et al.*<sup>5</sup> An energy-level diagram of ruby is shown in Fig. 1. This paper reports precise measurements of the excited-state absorption cross section in the visible and ultraviolet regions at temperatures of 40, 105, and 296°K. In addition to a sharpening of the bands at low temperatures, any difference between the matrix elements from the  $\bar{E}$  and  $2\bar{A}$  (the two states coming from  ${}^2E$ ) to the bands will also appear. At room temperature the population ratio of the  $\bar{E}$  and  $2\bar{A}$  (separated by  $\sim 29\text{ cm}^{-1}$ ) is 10:9, and at 40°K the ratio is 5:2, since these states are in thermal equilibrium.<sup>6</sup> Thus, a difference in the matrix elements will appear as a change in the absorption cross section.

## II. EXPERIMENTAL DETAILS

One sample was a Linde  $\sim 0.01\%$  ruby cylinder 1 cm in diameter and 3.9 cm in length with the optical axis perpendicular to the cylinder axis to within 3°. The other sample was 1 cm in length cut from the same cylinder. They have a  $\text{Cr}^{3+}$  concentration of  $4.43 \times 10^{18}/\text{cm}^3 \pm 3\%$  determined spectrophotometrically.<sup>7</sup> The ends of the sample are polished while the sides are left rough to aid in producing uniform pumping. As a further precaution, diaphragms were used so that the absorption measurement was made on the central part,

4 mm in diameter, of the rod cross section.<sup>8</sup> Optical pumping was performed in an elliptical cylinder reflector by a straight xenon flash-lamp which emitted a light pulse of about 1.0 msec duration. The probe light is a pulse of about 5  $\mu\text{sec}$  duration with an appropriate time delay. A half-meter Ebert spectrometer and gated RCA1P28, 7102, and C70128 photomultiplier detectors were used. The C70128 was a solar blind ultraviolet photomultiplier necessitated by the large amount of visible scattered light. The repeatability of the data of this system is better than  $\pm 1\%$  in the visible region. The statistical error of the measured absorption spectrum, expressed in terms of the excited-state cross section, was less than  $\pm 0.15 \times 10^{-20}\text{ cm}^2$  throughout the visible region (3000 to 7000 Å, Figs. 5-7) and was  $\pm 0.5 \times 10^{-18}\text{ cm}^2$  in the ultraviolet (Figs. 8 and 9). Details of this system have been published in another article.<sup>9</sup> The ruby rod was held by an evacuated glass tube inside a glass cryostat Dewar<sup>10</sup> (see Fig. 2) which can maintain a controlled temperature in the range from 30 to 300°K. At room temperature, the crystal specimen was cooled with dry nitrogen gas to avoid heating. At 105°K, the crystal was cooled with dry nitrogen gas passed through liquid nitrogen. At 40°K, cold helium gas from the liquid-helium Dewar was forced through the glass Dewar via a transfer tube and a gas vacuum pump at the outlet of the glass Dewar. A Glan prism was used as polarizer and polarization with respect to the ruby optical axis was obtained by rotating the polarizer to give maximum or minimum transmitted light intensity at 4000 Å. The polarization was oriented to the optical axis to better than  $\pm 2^\circ$ . Generally, the room-temperature data was taken at 25 Å intervals and the other temperatures at 50 Å intervals. However, critical-wavelength regions were taken at much smaller intervals.

## III. CALCULATION OF THE ABSORPTION OF THE EXCITED STATES

Let  $N_0$  be the number of  $\text{Cr}^{3+}$  ions per  $\text{cm}^3$ ,  $n$  the population of the ground state  ${}^4A_2$ , and  $n^*$  the number of ions in the metastable states. Let  $\sigma_0(\lambda)$  and  $\sigma^*(\lambda)$

† Supported by the U.S. Army Research Office-Durham, N.C.

\* Present address: Towson State College, Baltimore, Md.

‡ Alfred P. Sloan Foundation Research Fellow.

<sup>1</sup> T. H. Maiman, *Phys. Rev. Letters* **4**, 564 (1960).<sup>2</sup> F. Gires and G. Mayers, *J. Phys. Radium* **22**, 832 (1961); *Centre Rech. Acad. Sci.* **254**, 259 (1962); *Ann. Radioelec.* **18**, 112 (1963).<sup>3</sup> G. K. Klauminzer, P. L. Scott, and H. W. Moos, *Phys. Rev.* **142**, 248 (1966).<sup>4</sup> T. Kushida, *J. Phys. Soc. Japan* **21**, 1333 (1966).<sup>5</sup> M. Shinada, S. Sugano, and T. Kushida, *J. Phys. Soc. Japan* **21**, 1342 (1966).<sup>6</sup> D. F. Nelson and M. D. Sturge, *Phys. Rev.* **137**, 1117 (1965).<sup>7</sup> D. M. Dodd, D. L. Wood, and R. L. Barns, *J. Appl. Phys.* **35**, 1183 (1964).<sup>8</sup> G. E. Devlin, J. McKenna, A. D. May, and A. L. Schawlow, *Appl. Opt.* **1**, 11 (1962).<sup>9</sup> H. W. Moos, C. B. Opal, and J. W. Huang, *Appl. Opt.* **6**, 877 (1967).<sup>10</sup> J. W. Huang (unpublished).

be the effective absorption cross sections of  ${}^4A_2$  and the metastable state, respectively. If  $I_0$  is the intensity of the probe light incident on the ruby,  $I_u$  the intensity after traversing a length  $L$  of the ruby, in the absence of pumping, we have

$$\ln(I_0/I_u) = N_0\sigma_0(\lambda)L. \quad (1)$$

Let  $I_p$  be the intensity traversing the length  $L$  in the presence of pumping. Then

$$\ln(I_0/I_p) = [n\sigma_0(\lambda) + n^*\sigma^*(\lambda)]L. \quad (2)$$

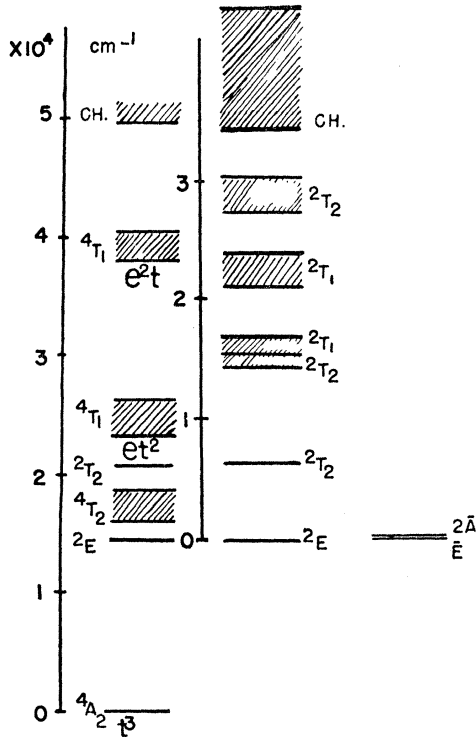


FIG. 1. Absorption energy levels of ruby observed from the  ${}^4A_2$  state (column one) and from  ${}^2E$  state (column two). The two states of  ${}^2A$  and  $E$  are separated by  $29.1 \text{ cm}^{-1}$  (column three). CH refers to charge transfer bands.

Thus, from Eq. (1), Eq. (2) and  $n+n^*=N_0$  we have

$$\ln(I_p/I_u) = n^*L[\sigma_0(\lambda) - \sigma^*(\lambda)]. \quad (3)$$

#### IV. EXCITED-STATE POPULATION

Two methods were used to measure the population distribution for a pumped ruby. Below  $200^\circ\text{K}$  there exists a series of narrow vibrational bands near the origin of the  ${}^4A_2 \rightarrow {}^4T_2$  transitions. There are no vibrational bands associated with the excited-state absorption (transition from  ${}^2E$ ). Hence the area under the vibronics can be used to measure the population. Let  $\sigma_v$  denote the absorption cross section of the vibrational sidebands; it is a function of both wavelength and temperature  $T$ .  $\sigma_0(\lambda)$  is taken not to include the vibrational sidebands. Then Eqs. (1) and (2) can be re-

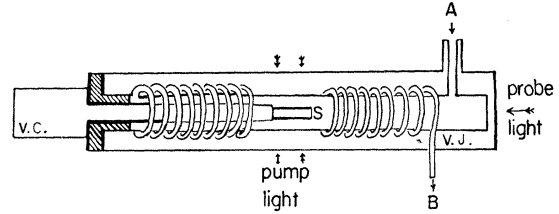


FIG. 2. Glass cryostat Dewar: Cold helium gas comes in through a vacuum-jacketed transfer tube at A passing over the sample S. It is then forced out through a vacuum pump at B. V.C. and V.J. stand for vacuum cell and vacuum jacket, respectively. The shaded area is a ground glass joint.

written as

$$\ln(I_0/I_u) = N_0\sigma_0(\lambda)L + N_0\sigma_v(\lambda, T)L, \quad (4)$$

$$\ln(I_0/I_p) = n\sigma_0(\lambda)L + n\sigma_v(\lambda, T + \Delta T)L + n^*\sigma^*(\lambda)L$$

$$= n\sigma_0(\lambda)L + n\sigma_v(\lambda, T) + \Delta\sigma(\lambda, T + \Delta T)L + n^*\sigma^*(\lambda)L, \quad (5)$$

where  $\Delta T$  is the difference in temperature of the crystal at the measurement of  $I_u$  and  $I_p$ , and  $\Delta\sigma$  is the change in vibrational cross section due to the change in temperature. The heating of the crystal after a single flash was measured by the thermocouple. It was found that  $\Delta T$  was a slowly varying function of time with a maximum  $\leq 4^\circ\text{K}$  going to zero 100 msec after the start of pumping. In order to measure  $\sigma_v(T + \Delta T)$ ,  $I_p$ 's were measured every  $1 \text{ \AA}$  across the first two vibronic sidebands with a delay time of 50 msec with respect to the start of the pump. Under these conditions we have

$$\begin{aligned} \ln(I_0/I_p) &= N_0\sigma_0(\lambda)L + N_0\sigma_v(\lambda, T + \Delta T)L \\ &= N_0\sigma_0(\lambda)L + N_0\sigma_v(\lambda, T)L \\ &\quad + N_0\Delta\sigma(\lambda, T + \Delta T)L. \end{aligned} \quad (5')$$

The areas under the first two vibronic sidebands of

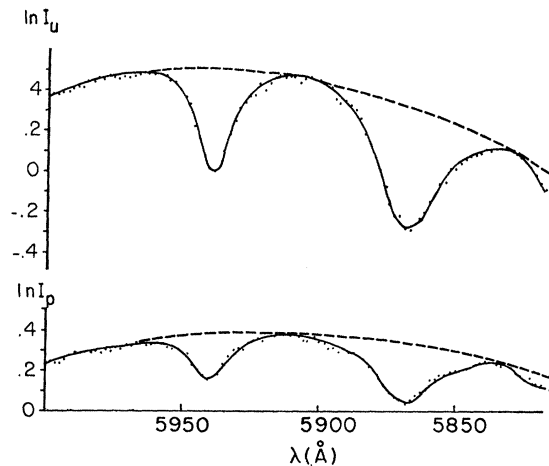


FIG. 3.  $\ln I_u$  of the first two vibronic sidebands of the  $({}^4A_2 \rightarrow {}^4T_2)$  transition in  $\sigma$  polarization at  $40^\circ\text{K}$ , and  $\ln I_p$  of the first two vibronic sidebands in  $\sigma$  polarization at  $40^\circ\text{K}$ .

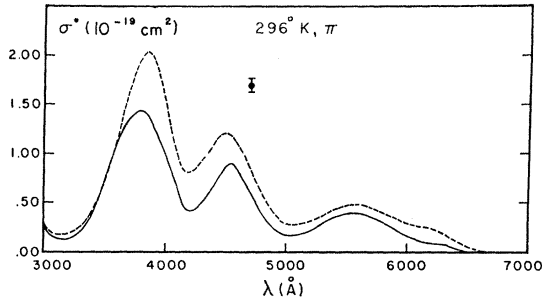


FIG. 4. Excited-state absorption cross section at 296°K. ( $\mathbf{E} \parallel C$ ) The results of Kushida (Ref. 4) are shown by the dotted line.

$I_u$  and  $I_p$  (with 50 msec delay) were compared with the result  $\Delta\sigma_v(T+\Delta T) \leq 1.5\%$  of  $\sigma_v$  at 100 and 40°K. Thus, we can neglect the term  $\Delta\sigma_v(T+\Delta T)$  in Eq. (5), and hence the ratio of the areas under the vibronic sidebands is equal to  $n/N$ . Experimental curves of  $\ln(I_u)$  and  $\ln(I_p)$  at 40°K are shown in Fig. 3. The data were taken at 1 Å intervals. From these we have  $n^* = (49 \pm 2)\%$  of  $N_0$  at 40°K and  $(49.5 \pm 3)\%$  at 100°K.

Since there are no vibronics at room temperature and the above method is not applicable, a ruby laser was used as the probe light.<sup>4</sup> The laser intensity was reduced so that it would not affect the population distribution of the crystal and its polarization was oriented with  $\mathbf{E}_\perp$  to the  $C$  axis of the sample. After the crystal is pumped, the transmitted laser light is given by<sup>11</sup>

$$I_p = I_0 \exp[L\sigma_0(\lambda)(n^* - n)]. \quad (6)$$

Combining this equation with Eq. (1) we have  $\ln(I_p/I_u) = 2\sigma_0(\lambda)n^*L$  at  $\lambda = 6943$  Å. Forty points of  $I_p/I_u$  were measured and gave  $n^* = (47.5 \pm 3.5)\%$  of  $N_0$ .

In the visible region, the accuracy of the excited-state cross section is set not by statistical variations in

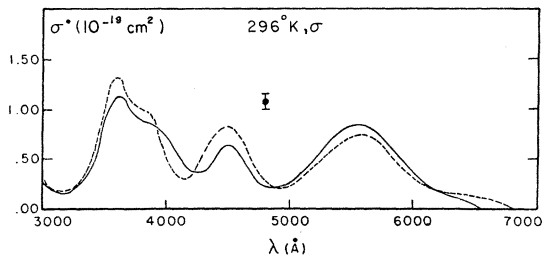


FIG. 5. Excited-state absorption cross section at 298°K ( $\mathbf{E} \perp C$ ). The results of Kushida (Ref. 4) are shown by the dotted line.

<sup>11</sup> After the crystal was pumped, the electrons were distributed among the five metastable states and ground state. Let  $n_1$  and  $n_2$  be the electron population of ground state and the lower state of  ${}^2E$ . Then

$$n_1 + n_2 [1 + \exp(-29.2 \text{ cm}^{-1}/kT) + \exp(-538 \text{ cm}^{-1}/kT) + \exp(-749 \text{ cm}^{-1}/kT)] = n_0$$

at  $T = 296^\circ\text{K}$  we have  $n_1 + n_2(1.99) = n_0$ . Then  $n^* = 2n_2$  to within 0.5%. Substituting this into

$$I_p = I_0 e^{-\sigma_0 L(n_1 - n_2/n_0)}$$

we have Eq. (6).

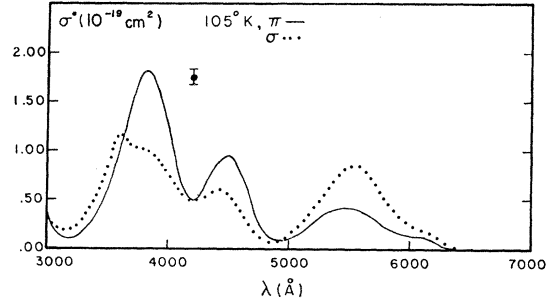


FIG. 6. Excited-state absorption cross section at 105°K. ( $\mathbf{E} \parallel C$ ) and ( $\mathbf{E} \perp C$ ).

the value of  $I_u/I_p$ , but by the determination of the excited-state population. If the value of the population were off by 10% (i.e., changed from 47.5 to 42.5%) the maximum change in the cross section would be  $0.15 \times 10^{-19} \text{ cm}^{-2}$ . Using this conservative value for the error bar on the population, the value of  $\pm 0.15 \times 10^{-19} \text{ cm}^{-2}$  is taken as an error bar on the cross-section measurements. In regions of low ground-state absorption, the error bars are smaller on the order of  $\pm 10\%$  of the excited-state cross section. In the ultraviolet region, the error bars of  $\pm 0.5 \times 10^{-18} \text{ cm}^{-2}$  are determined by statistical fluctuations in  $I_u$  and  $I_p$ . Once again, this value decreases away from the maximum absorption.

## V. EXPERIMENTAL RESULTS

The logarithms of the ratio of pumped transmitted intensity to unpumped transmitted intensity at three different temperatures and two different polarizations were plotted as functions of wavelength.  $\sigma^*(\lambda)$ 's were then derived by substituting for each case the proper ground-state absorption cross section  $\sigma_0$  and the excited-state population  $n^*$  corresponding to the  $I_p$  measurements. Figures 4–7 are plots of  $\sigma^*(\lambda)$  versus wavelength.

The lifetime of the excited state was measured by observing the fluorescence decay rate at various temperatures. The decay rate of  $\ln(I_p/I_u) = n^*L[\sigma_0(\lambda) - \sigma^*(\lambda)]$ , where  $n^* = n_0^* e^{-t/T}$  was determined in both the visible and ultraviolet at the extreme of  $\ln(I_p/I_u)$ . The results are given in Table I. In order to minimize errors such as those introduced by mismatch of wavelength and to obtain values of  $\sigma_0(\lambda)$  at the same temperatures at which the  $I_p$  measurements were made, the ground-state absorption spectrum was measured using the same apparatus. At room temperature the values of  $\sigma_0(\lambda)$  obtained agree within 1% with those obtained

TABLE I. Comparison of lifetimes of  $R$  line fluorescence and excited-state absorption (in msec).

	296°K	105°K	40°K
Fluorescence	$3.0 \pm 1.5$	$5.5 \pm 0.3$	$6.1 \pm 0.3$
Excited-state absorption	$3.1 \pm 0.2$	$5.3 \pm 0.4$	$6.2 \pm 0.3$

TABLE II. Positions, peak heights, and relative area under each excited-state absorption band in the visible and ultraviolet. Uncertainty in position is  $\pm 20 \text{ \AA}$ , except for those designated by + which are  $\pm 50 \text{ \AA}$ . The assignments are taken from Ref. 5. Ch refers to charge transfer band.

Assignment	Positions $\lambda(\text{\AA})$	296°K		105°K		40°K			
		Peak height ( $10^{-19}$ $\text{cm}^{-2}$ )	Relative area	Peak height ( $10^{-19}$ $\text{cm}^{-2}$ )	Relative area	Peak height ( $10^{-19}$ $\text{cm}^{-2}$ )	Relative area		
$E(1)$	6350 <sup>†</sup> ( $\sigma$ )	0.12	286	6200 <sup>†</sup> ( $\sigma$ )	0.14	249	6030 <sup>†</sup> ( $\sigma$ )	0.21	245
$E(2)$	5550 r( $\sigma$ )	0.84		5550 ( $\sigma$ )	0.85	5530 ( $\sigma$ )	0.92		
$E(1)$	6300 <sup>†</sup> ( $\pi$ )	0.07	129	6140 <sup>†</sup> ( $\pi$ )	0.12	129	6000 <sup>†</sup> ( $\pi$ )	0.15	131
$E(2)$	5550 ( $\pi$ )	0.40		5500 ( $\pi$ )	0.41		5500 ( $\pi$ )	0.42	
$E(3)A(3)$	4490 ( $\sigma$ )	0.63	107	4440 ( $\sigma$ )	0.60	105	4430 ( $\sigma$ )	0.57	104
$E(3)$	4530 ( $\pi$ )	0.85	167	4500 ( $\pi$ )	0.95	149	4500 ( $\pi$ )	1.00	147
$E(4)$	3900 <sup>†</sup> ( $\sigma$ )	0.83	291	3900 <sup>†</sup> ( $\sigma$ )	0.92	307	3900 <sup>†</sup> ( $\sigma$ )	1.00	333
$E(4)$	3610 ( $\sigma$ )	1.13		3610 ( $\sigma$ )	1.15		3620 ( $\sigma$ )	1.22	
$E(4)$	3800 ( $\pi$ )	1.43	334	3810 ( $\pi$ )	1.82	376	3810 ( $\pi$ )	2.08	425
Ch	2475 ( $\pi$ )	70	531				2450 ( $\pi$ )	89	534
Ch	2370 ( $\pi$ )	34		2360 ( $\pi$ )	45				
Ch	2475 ( $\sigma$ )	78	720				2425 ( $\sigma$ )	131	867

using a Cary model 14 spectrometer. In the uv region  $\sigma^*(\lambda)$  is about two orders of magnitude greater than  $\sigma_0(\lambda)$ . Hence  $\sigma_0(\lambda)$  is neglected in Eq. (3) in this region and the results are plotted in Figs. 8 and 9.

## VI. DISCUSSION

The results of both the visible and ultraviolet measurements are summarized in Table II. Relative areas under the various bands are given to show the changes in intensity with temperature.

The room-temperature values of  $\sigma^*(\lambda)$  in the visible are generally somewhat lower than those of Kushida,<sup>4</sup> except at one band (5500  $\text{\AA}$  in  $\sigma$  polarization). No estimates of error bars are given in his work. The  $\pi$ - $\sigma$  polarization ratio is also somewhat lower, on the order of 1.2 versus 1.5. It should be noted that Kushida used an optically thick sample of 5 cm length and 0.02%  $\text{Cr}^{3+}$  concentration. The small band reported at 6600  $\text{\AA}$

was not observed in this work, although there is definitely a band at 6350  $\text{\AA}$  corresponding to the band designated  $E(1)$ .<sup>5</sup>

Kiang *et al.*<sup>12</sup> have reported excited-state absorption cross sections for ruby between 4000 and 7000  $\text{\AA}$  at 115°K for  $\mathbf{E} \perp \mathbf{C}$ . Our results do not agree with theirs. However, their measurements were made every 100  $\text{\AA}$  and the excited-state population was determined by incorrectly assuming  $\sigma^*(\lambda)=0$  at  $\lambda=4100 \text{ \AA}$ . The extra bump near 5700  $\text{\AA}$  seen on their curves of both  $I_p/I_u$  and  $\sigma^*$  was not observed. Also, in the band at 4500  $\text{\AA}$ , we find that  $\sigma^* > \sigma_0$  whereas Kiang *et al.* report  $\sigma^* < \sigma_0$ . Owing to the high repeatability and resolution of our apparatus, we believe our result is correct.

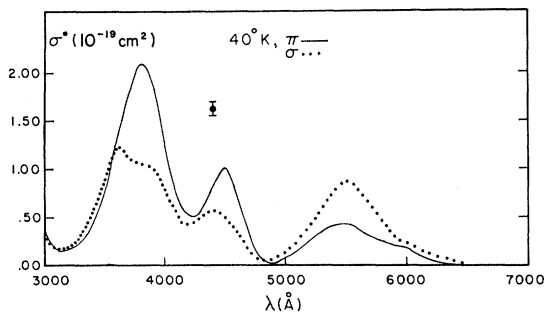


FIG. 7. Excited-state absorption cross section at 40°K. ( $\mathbf{E} \parallel \mathbf{C}$ ) and ( $\mathbf{E} \perp \mathbf{C}$ ).

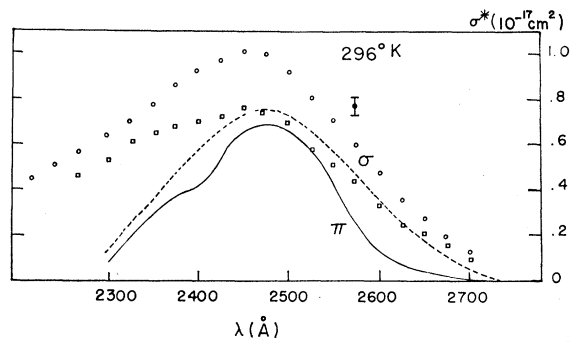


FIG. 8. Excited-state absorption cross section at 296°K (uv). The squares were taken from Kushida's curve (Ref. 4) in  $\pi$  polarization. The circles were taken from Kushida's curve in  $\sigma$  polarization.

<sup>12</sup> Y. C. Kiang, J. F. Stephany, and F. C. Unterleitner, J. Quantum Electron. 1, 295 (1965).

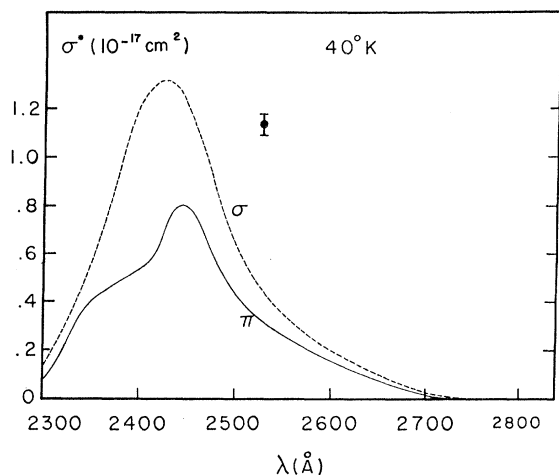


Fig. 9. Excited-state absorption cross section at 40°K (uv).

The ultraviolet bands measured here are shown in Figs. 8 and 9. The short-wavelength side in our work drops somewhat faster than Kushida's. The  $\pi$  ultraviolet bands appear at longer wavelengths and have a somewhat different shape. A similar ultraviolet absorption band from the  ${}^2E$  state of  $\text{Cr}^{3+}$  in  $\text{MgO}$  was also found at  $\lambda = 2800 \text{ \AA}$ .<sup>13</sup> The peak height of this band is  $\sigma^* = (55 \pm 25) 10^{-19} \text{ cm}^2$  and the cross sections for the  ${}^4T_1$  and  ${}^4T_2$  states are  $6.9 \times 10^{-20}$  and  $2.1 \times 10^{-20} \text{ cm}^2$ , assuming the manufacturer's nominal concentration. The ratio of the uv cross section to the average of the two visible cross sections is 120. This is to be compared with  $\text{Al}_2\text{O}_3:\text{Cr}^{3+}$ , which has an average ratio of 30. Although the  $\text{MgO}:\text{Cr}^{3+}$  ultraviolet cross section has an uncertainty due to concentration, both  $\text{MgO}:\text{Cr}^{3+}$  and  $\text{Al}_2\text{O}_3:\text{Cr}^{3+}$  ultraviolet band cross sections are of the same order of magnitude, indicating the similarity of the mechanism for the charge transfer bands in both cases.

Table II shows that the  $3800 \text{ \AA}$  ( $\pi$ ) band increases in area by 27% between 296 and 40°K. The nearby band at  $4530 \text{ \AA}$  shrinks slightly, but this is not sufficient to explain the increase in intensity as being borrowed from the band. Other visible bands show smaller changes. The  $2475 \text{ \AA}$  ( $\sigma$ ) band in the ultraviolet also changes, increasing by 19% between 296 and 40°K. McClure<sup>14</sup> has shown that changes in intensity due to the Franck-Condon principle are expected to be small between 296 and 77°K. Cooling the crystal decreases the fraction of excited ions in states above the  $\bar{E}$  and  $2\bar{A}$  states. However, only 10% are in these higher states at 296°K and

<sup>13</sup> J. W. Huang, Ph.D. dissertation, Johns Hopkins University 1968 (unpublished).

<sup>14</sup> Donald S. McClure, *J. Chem. Phys.* **36**, 2757 (1962).

cooling cannot explain the 27% increase in band intensity. Therefore, it is felt that these changes in intensity are due to differences in transition strengths from the  $\bar{E}$  and  $2\bar{A}$  states to these states, and the variation in the population ratio of the  $\bar{E}$  and  $2\bar{A}$  states with temperature. One can make a rough comparison of the  $\bar{E}$  and  $2\bar{A}$  transition matrix elements based on the fact that a Boltzmann distribution exists among the five states of  ${}^2E(t_2^3)$  and  ${}^2T_1(t_2^3)$ . Since the  ${}^2T_1$  states are much less populated than the  ${}^2E(t_2^3)$  state and the dipole strengths for the transitions initiating from  ${}^2T_1$  and  ${}^2E$  are comparable, the initial states of excited-state absorption were taken as  $\bar{E}$ ,  $2\bar{A}$  of  ${}^2E$ , and the lowest state  $\bar{E}'$  of  ${}^2T_1$ .

Let  $n'$  be the population of  $\bar{E}$ . Then

$$n' \exp(-29 \text{ cm}^{-1}/kT)$$

is the population in the state  $2\bar{A}$ , and

$$n' \exp(-539 \text{ cm}^{-1}/kT)$$

the population in state  $\bar{E}'$ . If  $M_{1i}$ ,  $M_{2i}$ , and  $M_{3i}$  are the transitions from these  $\bar{E}$ ,  $2\bar{A}$ , and  $\bar{E}'$  states, respectively, to a higher state designated  $i$ , then

$$\sigma_T^*(i) \propto n_T' [M_{1i} + M_{2i} \exp(-29 \text{ cm}^{-1}/kT) + M_{3i} \exp(-538 \text{ cm}^{-1}/kT)].$$

Under the condition that the total populations of the metastable states are the same at different temperatures ( $T = 296, 105, \text{ and } 40^\circ\text{K}$ ), we have

$$\frac{\sigma_{40}^*}{\sigma_{105}^*} = \frac{1.44M_{1i} + 0.50M_{2i}}{1.17M_{1i} + 0.77M_{2i}},$$

and

$$\frac{\sigma_{40}^*}{\sigma_{296}^*} = \frac{1.44[M_{1i} + 0.35M_{2i}]}{M_{1i} + 0.87M_{2i} + 0.08M_{3i}}.$$

At  $\lambda = 3800 \text{ \AA}$ ,  $\mathbf{E} \parallel \mathbf{C}$ , we have from Table II

$$\sigma_{40}^*/\sigma_{296}^* = 1.27 \quad \text{and} \quad \sigma_{40}^*/\sigma_{105}^* = 1.13,$$

using the integrated area rather than the peak cross sections. Most of the error in the absolute cross section is due to uncertainties in the number of  $\text{Cr}^{3+}$  per cc. This error divides out in the ratio and the error of the ratios are  $\pm 5\%$ . Neglecting  $M_{3i}$  (inclusion of which would increase the result) we obtain  $(M_{2i}/M_{1i}) \sim 3$  for the two ratios above. The change in absorption with temperature is relatively insensitive to the ratio of the matrix elements. For instance, using these relative values for  $M_{1i}$  and  $M_{2i}$ , one would expect about a 35% change of  $\sigma^*$  in this region by going from liquid-nitrogen to liquid-helium temperatures.